Acta Chemica Scandinavica, 1998: 52: 718–727
Printed in UK - all rights reserved

ACTA
CHEMICA SCANDINAVICA
ISSN 0904–213X

Angular Bond Flexibility and Closed-Shell Metal–Metal Interaction in Polymetal Copper(I), Silver(I) and Gold(I) Iodide Complexes. A Quantum Chemical Study

P. Alemany,[a] L. Bengtsson-Kloo[b,*] and B. Holmberg[b]

[a]Department of Physical Chemistry, University of Barcelona, Diagonal 647, 08028 Barcelona, Catalunya, Spain and [b]Inorganic Chemistry 1, Lund University, PO Box 124, S-221 00 Lund, Sweden

Alemany, P., Bengtsson-Kloo, L. and Holmberg, B., 1998. Angular Bond Flexibility and Closed-Shell Metal–Metal Interaction in Polymetal Copper(I), Silver(I) and Gold(I) Iodide Complexes. A Quantum Chemical Study. – Acta Chem. Scand. 52: 718–727. © Acta Chemica Scandinavica 1998.

An applied theoretical study has been performed on the conformations of polymetal iodide complexes of the monovalent coinage metals at *ab initio* and semi-empirical level. The polysilver systems $[Ag_mI]^{m-1}$ ($m=1$–4) appear to be quite flexible, although the difference as compared to the corresponding copper(I) and gold(I) complexes is only of a quantitative nature. The results thus suggest that X-ray scattering data of formal $[Ag_4I]^+$ in aqueous solution and molten nitrate media are best described by assuming a high intramolecular Ag^+ mobility, indicating a direct connection between molecular polysilver complex properties and the bulk properties of Ag^+-conducting, solid materials. The polymetal complexes have an overall tendency to prefer bent conformations with short metal–metal separations. No direct covalent interaction between the metal ion ligands can be detected, and although a stabilisation by dispersion interaction cannot be excluded, the results are adequately described by second-order Jahn–Teller interaction at the central iodide ion; the bent conformations allowing a stabilisation through iodine sp-mixing.

The coordination compounds of silver with the halides have been of interest to both solution and solid-state chemists for at least 50 years. The increase in solubility of the silver halides in aqueous halide solutions was interpreted in terms of a stepwise anionic complex formation, $[Ag_mX_n]^{-(n-m)}$, ($n>m$; $n=1$–4). The silver halides are almost unique in the sense that the solubility of AgX also increases in solutions with an excess of Ag^+ ions, owing to the formation of polymetal complexes of the formal composition $[Ag_mX]^{m-1}$ ($m>1$). Pioneering thermodynamic studies were done in aqueous solution by Leden and Lieser, and later in ionic liquid media by Holmberg.[1–4]

The subsequent liquid structural studies employing X-ray scattering on solutions and melts optimised in $[Ag_4I]^{3+}$ (and $[Ag_4Br]^{3+}$), based on the thermodynamic results, gave some unexpected results: the radial distribution functions display a peak corresponding to the Ag–I (and Ag–Br) distances, but remarkably no other significant features; most notably no distinct Ag–Ag correlation. Integration of the Ag–I peak showed that it corresponds to approximately four such distances per I^-, although the error in the estimation of the number of atom–atom vectors is quite high (20–30%).[5,6]

At about 146 °C AgI is transformed into its α-form. In α-AgI iodine is bcc packed, whereas the silver ions apparently move with a very low activation barrier between several crystallographic positions; the compound is one of the best known superionic conductors with a conductivity around 1 $\Omega^{-1}\,cm^{-1}$. Also compounds such as Ag_2HgI_4 and various silver-halide-doped glasses with isolated and network-forming oxoanions are excellent silver-ion conductors. The latter systems are analogous to the polymetal $[Ag_mX]^{m-1}$ systems studied in solution, at least when comparing the relative silver to halide ion concentration and predominating molecular structural fragments; thus a link seems to exist between the molecular properties found in solution and the bulk properties of the solid ion-conducting materials.

The structural chemistry of polymetal complexes of gold(I) has recently rendered special attention because of the so-called 'aurophilic' interaction, in which polygold complexes assume unexpected configurations with short metal–metal separations around main-group coordination centres.[7] Similar arrangements have also been observed for the other coinage metals in the formal +I oxidation state.[8–10]

These systems have been studied theoretically at semi-empirical, density-functional and *ab initio* levels, giving

* To whom correspondence should be addressed.

rise to two conflicting bonding models for explaining the tendency towards a short metal–metal separation. The semi-empirical and density-functional results indicate that direct metal–metal orbital interactions overcome the formal gold(I)–gold(I) repulsion, whereas post-Hartree–Fock methods invoking scalar relativistic effects suggest that the interaction is purely a correlation effect (i.e. dispersion) enhanced by relativity and thus increasing in the order Cu < Ag < Au.[11] A recent review clearly shows that the tendency towards a strong closed-shell interaction is a characteristic property of the heavy elements with d^{10} and $d^{10}s^2$ valence configurations.[12]

The $[Ag_2I]^+$ unit deserves special attention, since it is the fundamental structural unit in the tetrahedral entities that build up Ag^+ ion conducting materials and glasses. The isoelectronic and neutral Cu_2Se complex is the smallest structural unit in the large Cu–Se clusters of Fenske and co-workers. Recently, such units have theoretically been shown to be bent with a very soft Cu–Se–Cu bending potential,[13–15] in analogy to our previous results for $[Ag_2I]^+$, Ag_2Se, $[Au_2I]^+$ and Au_2Se.[16] Similar high-level calulations on Ag_2S and Au_2S show a preference for a bent configuration with rather short metal–metal separations. The metal–metal interaction was shown to be predominantly of the dispersion type, although large-core effective core potentials (ECPs) overemphasize this effect.[17]

The present study includes an applied theoretical analysis at both the *ab initio* level, employing the pseudopotential approximation, and at the semi-empirical level of the polymetal iodide complexes of the monovalent coinage metals. The study focuses on the intramolecular flexibility of the polymetal complexes and the potential link to solid superionic conductors. The complex stabilisation through metal–metal dispersion interaction is also addressed.

Calculational details

Most calculations in this work were made with the LANL2DZ basis sets of Gaussian92/94 employing ECPs for the heavier atoms and full double-zeta basis sets for H, N, O and F.[18–20] The LANL2DZ ECP basis sets are essentially the original small-core ECP basis sets published by Hay and Wadt supplemented with an additional p-function for the fifth- and sixth-row elements. In the comparative study of dimetal iodide species of groups 11 and 12, the LAN1DZ basis sets were used employing the large-core ECPs for the transition metals. In a preliminary study on dimetal $[M_2X]^{+/0}$ (M = Ag, Au; X = I, Se) these ECP basis sets were shown to give consistent results comparable to those emerging from non-relativistic, *ab initio* all-electron calculations.[16]

Scalar relativistic effects are accounted for indirectly by the use of average relativistic ECPs. In this study the transition metals have a formal closed-shell d^{10} valence configuration. Several studies have shown that ECP-based basis sets perform as well as all-electron ones for most properties of both open- and closed-shell molecules.[21] Hartree–Fock (HF) calculations tend to give rather realistic results, but the instantaneous electron–electron correlation was taken into account by employing Møller–Plesset perturbation theory to the second-order (MP2). The exchange and correlation functionals used in density-functional theory are normally derived on the basis of the shape of the exchange-correlation hole within the electron gas formalism, and therefore a typical DFT method based on the functionals of Becke and of Lee, Yang and Parr (BLYP) was included for sake of comparison.[22–24]

In order to analyze the bonding in these compounds from a qualitative point of view we have also performed calculations using the extended Hückel method. Although bonding models so far postulated for compounds containing d^{10} cations differ greatly in detail, they all lead to the same conclusion: the presence of a low-lying excited state destroys the pure 'core' nature of the closed d^{10} shell and also destroys its spherical symmetry. Since the d–s separation is clearly of central importance in this respect, the parameters used in a semi-empirical model must be carefully chosen in order to reproduce the structural and dynamical behavior found experimentally for the different coinage metals. Using the standard valence shell ionization potential, $H_{ii}(d) = -14$ eV, for copper as a reference and the energy separations indicated in Table 1, one can derive the H_{ii} values shown in Table 2 for all three metal atoms.[25]

Since our main aim in using the extended Hückel method is to understand the influence of the d–s and d–p separations in the angular flexibility of the polymetal cations, we have simplified our models by taking the same principal quantum numbers and orbital exponents for all three metals. Our calculations were thus performed with the standard 4s, 4p and 3d Slater-type orbitals used for copper.[26] The extended Hückel parameters used for iodine are those given in Ref. 27.

Table 1. Experimental energy separations (in cm^{-1}) for the free M^+ ions.

M^+	$^1S_0$ ($d^{10}s^0$) → $^3D_3$ (d^9s^1)	$^1S_0$ ($d^{10}s^0$) → $^3P_2$ (d^9p^1)
Cu^+	21928	66418
Ag^+	39163	80172
Au^+	15039	63052

Table 2. Valence shell ionisation potentials (in eV) used in the extended Hückel calculations.

M^+	H_{ii}(s)	H_{ii}(p)	H_{ii}(d)
Cu^+	−11.28	−5.77	−14.0
Ag^+	−9.14	−4.06	−14.0
Au^+	−12.14	−6.18	−14.0

Results and discussion

Non-solvated complexes. The thermodynamics and structures of the polysilver iodide and bromide systems, formally formulated as $[Ag_mX]^{m-1}$ (**1**–**4**), have been studied in both concentrated aqueous solution and ionic liquids. The experimental knowledge about these systems thus serves as calibration for our theoretical studies.

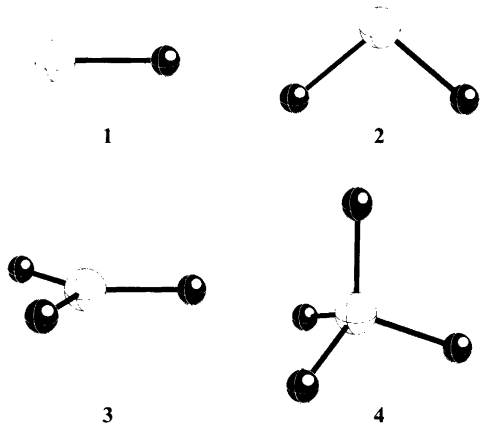

Of course, the 'naked' notation used is a gross oversimplification, and the ionic nature of the solvent definitely is of fundamental importance for the stabilisation of polymetal complexes or clusters with high formal positive charge. This fact is nicely illustrated by the results collected in Table 3. The MI and $[M_2I]^+$ (M = Cu, Ag, Au) entities have optimised M–I distances close to those observed for the monovalent solids, gaseous MI, various anionic complexes and the structurally characterised formal $[Ag_4I]^{3+}$ ion in both aqueous solution and nitrate melts, as seen in Table 4. The attachment of more than two cations to the central iodide ion gives rise to substantially longer optimised M–I distances in the D_{3h} and T_d point groups.

Table 5 contains the comparative results for the group 11 and group 12 $[M_2I]^{+/3+}$ ions. The dimetal complexes of the group 12 metal ions have M–I distances known from the solids MI_2(s), gaseous MI_2, and solution species such as $[CdI]^+$ and $[Hg_2I]^{3+}$ collected in Table 4. Generally, the optimised M–I–M angle is slightly larger for the group 12 dimers than for the corresponding group 11 ones, possibly reflecting the larger cation–cation repulsion.

The potential energy curves (M–I distance optimised at fixed M–I–M angles between 80 and 180°) for M–I–M bending are shown in Figs. 1a and 1b. For both groups the bent configuration is energetically preferred in spite of the obvious cation–cation electrostatic repulsion. The dimetallic complexes of group 11 metal ions have very flat potential curves, both in comparison with the corresponding group 12 congeners and thermal energy (almost 0.03 eV) at room temperature. The most shallow potential curve is found for silver(I) and cadmium(II) in the two groups. The isoelectronic Cu_2Se molecule studied by Alrichs and co-workers also exhibits a flat potential curve for angular deformation. The heaviest group members deviate the most, as seen by more steep potential curves and minima at smaller angles; gold(I) is here anomalous with a minimum at about 69°. The M–M

Table 3. Calculational results for the non-solvated $[M_mI]^{m-1}$ complexes employing the LANL2DZ basis sets.

M =	Cu		Ag		Au	
	HF	MP2	HF	MP2	HF	MP2
[MI]						
R_{M-I}/Å	2.505	2.455	2.715	2.673	2.647	2.622
$[M_2I]^+$						
R_{M-I}/Å	2.622	2.545	2.848	2.776	2.737	2.682
Λ_{M-I-M}/°	124.2	104.6	129.1	110.8	107.0	74.1
Opt. symm.	C_{2v}	C_{2v}	C_{2v}	C_{2v}	C_{2v}	C_{2v}
ΔE/eV[a]	0.084	0.267	0.053	0.196	0.408	0.854
$[M_3I]^{2+}$						
R_{M-I}/Å	2.817	2.702	3.056	2.946	2.930	2.813
Λ_{M-I-M}/°	120.0	120.0	120.0	120.0	120.0	103.4
Opt. symm.	D_{3h}	D_{3h}	D_{3h}	D_{3h}	D_{3h}	C_{3v}
ΔE/eV[b]						0.120
$[M_4I]^{3+}$						
R_{M-I}/Å	3.286	3.008	3.527	3.268	3.302	2.998
Λ_{M-I-M}/°	109.5	109.5	109.5	109.5	109.5	109.5
Opt. symm.	T_d	T_d	T_d	T_d	T_d	T_d
ΔE/eV[c]	0.635	0.670	0.585	0.635	0.646	0.841

[a] Energy favouring the freely optimized structure (C_{2v}) relative to the restricted structure with Λ_{M-I-M} frozen at 180° ($D_{\infty h}$). [b] Energy favouring the freely optimized structure (C_{3v}) relative to the restricted structure with Λ_{M-I-M} frozen at 120° (D_{3h}). [c] Energy favouring the freely optimized structure (T_d) relative to the restricted structure with Λ_{M-I-M} frozen at 90° (D_{4h}).

Table 4. Experimental structural data for solid, liquid and gaseous group 11/12 metal–iodide compounds with low coordination numbers for iodine.

Compound[a]	Iodine coord. number	R_{M-I}/Å	Ref.
CuI(g)	1	2.34	28
CuI(s)-α	4	2.51–2.65	29
CuI(s)-β	4	2.56–3.10	
CuI(s)-γ	4	2.61	
Cu_2HgI_4(s)-α	3	2.64(Cu), 2.65(Hg)	30
Cu_2HgI_4(s)-β	3	2.63(Cu), 2.80(Hg)	
$Cu_3P_{15}I_2$(s)	4[b]	2.58–2.68	31
$[Cu_2I_4]^{2-}$(s)	1; 2	2.49–2.51; 2.57–2.61	32
$[Ag_2Cu_2I_8]^{4-}$(s)	1; 2	2.58(Cu); 2.60(Cu), 2.82–2.95(Ag)	33
$[Cu_2I_4]^{2-}$(dmso)	1; 2	2.54	34
$[Cu_2I_4]^{2-}$(mecn)	1; 2	2.59	
AgI(g)	1	2.54	35
AgI(s)-α	4	2.83	36
AgI(s)-β	4	2.80–2.82	37
Ag_2HgI_4(s)-α	3	2.59–2.96(Ag, Hg)	38
Ag_2HgI_4(s)-β	3	2.81–2.82(Ag), 2.78(Hg)	39
$Ag_2I(NO_3)$(s)	4+2[c]	2.86–3.10	40
$Ag_3I(NO_3)_2$(s)	4+2[c]	2.84–3.08	41
$Ag_2HgI_2(NO_3)_2 \cdot H_2O$(s)	3	2.71–3.11(Ag), 2.63(Hg)	42
$Ag_2IF \cdot H_2O$(s)	4[b]	2.81–2.90	43
$[Ag_2I_4]^{2-}$(s)	1; 2	2.67; 2.79–2.80	44
$[Ag_4I_8]^{4-}$(s)	1; 2[d]	3.17–3.19; 2.76–2.99	45
$[Ag_4I_8]^{4-}$(s)	1; 2[e]	2.69–2.82; 2.90–2.93	46
$[AgI_2]_n^-$(mecn)	2	2.81	47
$[AgI(tht)]_4$(tht)	3[f]	2.82	48
$[Ag_4I]^{4+}$(aq)	4	2.79	5
$[Ag_4I]^{4+}$(melt)	4	2.80	6
AuI(s)	2	2.62	49
$[AuI_2]^-$(s)	2	2.53–2.54	50
ZnI_2(g)	2	2.38	51
ZnI_2(s)	2	2.57–2.67	52
CdI_2(g)	2	2.55	51
CdI_2(s)	3	2.98–2.99	53
$[CdI]^+$(aq)	1	2.77	54
HgI_2(g)	2	2.61	51
HgI_2(s)-red, orange, yellow	2	2.61–2.79	55
$HgI(NO_3)$(s)	2[d]	2.64, 2.66	56
$Hg_2I_2(TiF_6)$(s)	2[d]	2.62, 2.63	57
$[HgI_2]$(dmso)	2	2.62	58
$[Hg_2I]^{3+}$(aq)	2	2.63	59
$[Hg_2I]^{3+}$(dmso)	2	2.61	

[a] aq, water; dmso, dimethyl sulfoxide; mecn, acetonitrile; tht, tetrahydrothiophene; melt, nitrate ionic liquid. [b] Pyramid. [c] Trigonal prism. [d] Chain. [e] Cube. [f] Stella quadrangular.

overlap populations are in all cases zero or slighly negative, indicating that the preferred bent geometry can not be assigned to metal–metal interaction by direct orbital overlap.

Models of solvation. Experimentally, a strong ionic medium is required to stabilise the polysilver clusters of formal high cationic charges, viz. $[Ag_4I]^{3+}$. The media used are based on nitrate (NO_3^-) or perchlorate (ClO_4^-), and the non-complexed silver cations have been shown to coordinate four oxoanions in a bidentate, asymmetric configuration. Thermodynamic, vibrational spectroscopic and direct structural results show that complex formation with anions such as I^- and Br^- is associated with a release of anions, qualitatively and quantitatively. It is difficult to uniquely interpret the data in terms of a change of coordination mode or number; probably both effects are significant. The results are in any case clear: the cations are preferably coordinated to the anions of the ionic medium, rather than any molecular constituent present, and the net coordination of the silver(I) cations is decreased upon binding to the halide centres.

Therefore, we have modelled the solvation by using anions such as H^-, F^-, Cl^- and NO_3^- in different conformations. Since we only have experimental polymetal structural information for the formal complexes $[Ag_4I]^{3+}$, the comparative study was confined to the silver systems $[Ag_mI]^{m-1}$. To each silver atom one, two

Table 5. Calculational results for the non-solvated dimetal $[M_2I]^{+/3+}$ complexes employing the LANL1DZ basis sets.

	R_{M-I}/Å		Λ_{M-I-M}/°		Optimum symmetry		ΔE/eV[a]	
	HF	MP2	HF	MP2	HF	MP2	HF	MP2
$[Cu_2I]^+$	2.622	2.552	124.8	103.7	C_{2v}	C_{2v}	0.080	0.258
$[Ag_2I]^+$	2.827	2.765	128.4	108.2	C_{2v}	C_{2v}	0.056	0.202
$[Au_2I]^+$	2.748	2.706	108.1	68.9	C_{2v}	C_{2v}	0.353	0.831
$[Zn_2I]^{3+}$	2.752	2.770	132.9	124.2	C_{2v}	C_{2v}	0.198	0.435
$[Cd_2I]^{3+}$	2.856	2.839	136.9	126.2	C_{2v}	C_{2v}	0.126	0.344
$[Hg_2I]^{3+}$	2.873	2.862	123.8	115.7	C_{2v}	C_{2v}	0.491	0.904

[a] Energy favouring the freely optimized structure (C_{2v}) relative to the restricted structure with Λ_{M-I-M} frozen at 180° ($D_{\infty h}$).

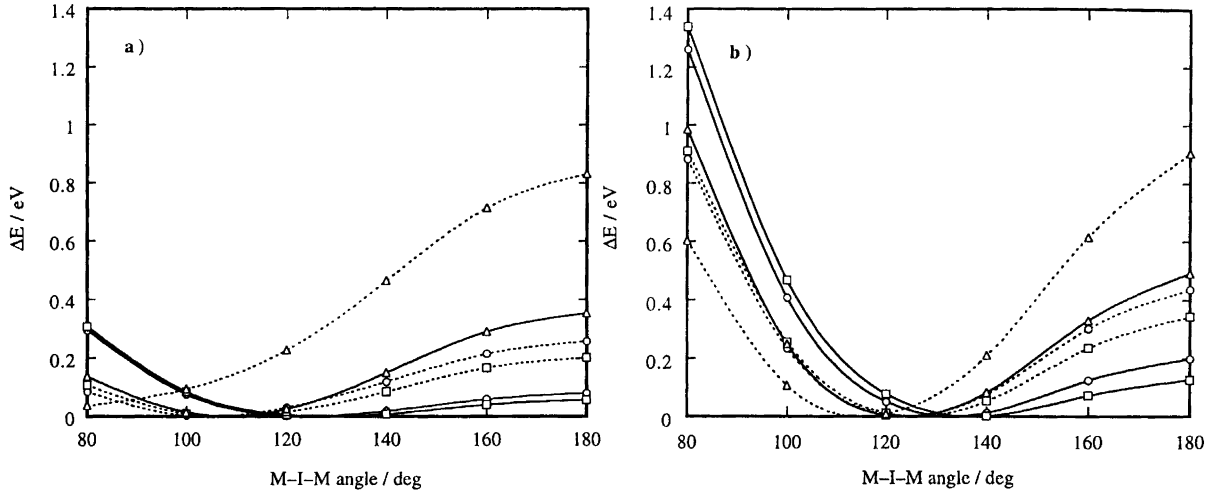

Fig. 1. The potential energy curves for M–I–M bending (optimised M–I distances at fixed angles) for (a) group 11 $[M_2I]^+$ complexes and (b) group 12 $[M_2I]^{3+}$ complexes. Circles represent Cu/Zn, squares Ag/Cd and triangles Au/Hg. Solid curves connect data points from HF calculations and hatched lines those from MP2 calculations.

or three solvent ions were attached. Only one non-bridging solvent ion per silver atom gives rise to realistic Ag–I distances for the tri- and tetrasilver complexes, the experimental Ag–I distance being our calibrator. It was also noted that all four model solvent ions give very similar results, making each of them eligible for further studies. The hydride and fluoride ions can potentially produce spurious results because of a strong tendency to dimerise, and the nitrate ions give rise to unnecessarily large calculations. Consequently, the chloride ion was chosen as a compromise for the complete study of solvation effects, $[M_mICl_m]^-$ being the object of study for all three metals in group 11.

How realistic is a solvent model based on one chloride ion per metal atom? As mentioned above, experimental results in nitrate and perchlorate ionic media indicate an effective solvent anion coordination number substantially lower than four in the formally cationic complexes. Furthermore, the high formal charge of an $[Ag_4I]^{3+}$ entity is unrealistic in a condensed medium, and would for instance not be expected to be found in a mass-spectroscopic experiment; a charge of +1 or −1 is more realistic, corresponding to $[Ag_4I(Ox)_2]^+$ or $[Ag_4I(Ox)_4]^-$ ($Ox = NO_3^-$ or ClO_4^-). We have chosen to explore the latter model, since we experimentally observe only one type of well defined Ag–I interaction (i.e. distance in the radial distribution functions), indicating that all four silver(I) atoms are coordinatively equivalent. The use of Cl^- to model solvent oxoanions seems electronically adequate, although the potential steric hindrance that might occur between the bulkier oxoanions is not properly handled by the monoatomic anion.

Solvated complexes. The results from the calculations of the structural properties of $[MICl]^-$, $[M_2ICl_2]^-$, $[M_3ICl_3]^-$ and $[M_4ICl_4]^-$ are shown in Table 6. The monomeric $[MICl]^-$ species in all cases display a linear (C_{iv}) configuration **5** with M–I distances of the correct magnitude.

The $[M_2ICl_2]^-$ dimers have a preferred bent configuration. The energy difference between the linear ($D_{\infty h}$) **6** and bent (C_{2v}) **7** configurations is higher than for the corresponding non-solvated ions (**2**). The energy difference is fairly low, but definitely larger than thermal energy at room temperature, and thus the dimeric complexes seem less floppy when anion solvation is taken into account. The energy difference is smallest for the silver complex; it is slightly larger for the copper dimer and substantially larger for the gold one, following the same trend as the naked $[M_2I]^+$ models.

Table 6. Calculational results for the solvated model $[M_mICl_m]^-$ complexes employing the LANL2DZ basis sets.

M =	Cu			Ag			Au		
	HF	BLYP	MP2	HF	BLYP	MP2	HF	BLYP	MP2
$[MICl]^-$									
R_{M-I}/Å	2.610	2.538	2.532	2.821	2.756	2.747	2.722	2.714	2.679
R_{M-Cl}/Å	2.280	2.230	2.229	2.513	2.434	2.472	2.463	2.438	2.443
Λ_{I-M-Cl}/°	180.0	180.0	180.0	180.0	180.0	180.0	180.0	180.0	180.0
$[M_2ICl_2]^-$									
R_{M-I}/Å	2.659	2.557	2.560	2.880	2.801	2.783	2.759	2.734	2.712
R_{M-Cl}/Å	2.256	2.213	2.208	2.485	2.436	2.446	2.432	2.434	2.415
Λ_{M-I-M}/°	106.7	88.7	76.2	113.3	104.8	85.8	105.3	105.9	71.6
Λ_{I-M-Cl}/°	176.1	172.1	172.6	174.8	177.3	173.9	177.0	177.5	174.2
Optimum symmetry	C_{2v}	C_{2v}	C_{2v}	C_{2v}	C_{2v}	C_{2v}	C_{2v}	C_{2v}	C_{2v}
ΔE/eV[a]	0.133	0.337	0.341	0.114	0.312	0.264	0.356	0.595	0.660
$[M_3ICl_3]^-$									
R_{M-I}/Å	2.709	2.598	2.588	2.947	2.847	2.820	2.801	2.801	2.770
R_{M-Cl}/Å	2.238	2.190	2.193	2.467	2.415	2.430	2.412	2.403	2.400
Λ_{M-I-M}/°	120.0	120.0	72.1	112.5	106.0	78.6	104.3	104.0	66.7
Λ_{I-M-Cl}/°	180.0	180.0	167.4	177.9	174.2	169.8	177.2	175.2	168.9
Optimum symmetry	D_{3h}	D_{3h}	C_{3v}	C_{3v}	C_{3v}	C_{3v}	C_{3v}	C_{3v}	C_{3v}
ΔE/eV[b]			0.286	0.007	0.083	0.131	0.098	0.196	0.485
$[M_4ICl_4]^-$									
R_{M-I}/Å	2.768	2.725	2.625	3.021	2.933	2.869	2.844	2.895	2.794
R_{M-Cl}/Å	2.224	2.200	2.180	2.453	2.418	2.415	2.399	2.421	2.388
Λ_{M-I-M}/°	109.5	58.1	67.3	109.5	63.6	69.7	109.5	63.0	65.2
Λ_{I-M-Cl}/°	180.0	162.3	167.0	180.0	171.2	168.8	180.0	170.6	170.5
Optimum symmetry	T_d	C_{4v}	C_{4v}	T_d	C_{4v}	C_{4v}	T_d	C_{4v}	C_{4v}
ΔE/eV[c]		0.488	0.218		0.198	0.023		0.260	0.489
ΔE/eV[d]		0.808	0.592		0.423	0.324		0.876	1.275

[a] Energy favouring the freely optimized structure (C_{2v}) relative to the restricted structure with Λ_{M-I-M} frozen at 180° ($D_{\infty h}$).
[b] Energy favouring the freely optimized structure (C_{3v}) relative to the restricted structure with Λ_{M-I-M} frozen at 120° (D_{3h}).
[c] Energy favouring the freely optimized structure (C_{4v}) relative to the restricted structure with Λ_{M-I-M} frozen at 109.5° (T_d).
[d] Energy favouring the freely optimized structure (C_{4v}) relative to the restricted structure with Λ_{M-I-M} frozen at 90° (D_{4h}).

5

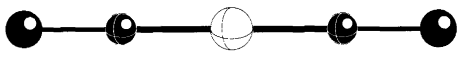

6

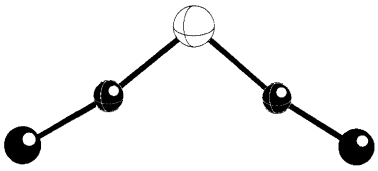

7

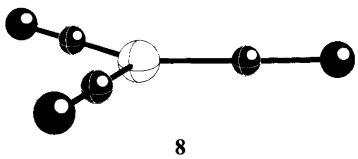

8

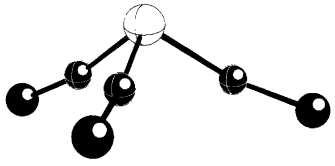

9

Also the trimeric clusters exist in two symmetrical forms: planar (D_{3h}) **8** and pyramidal (C_{3v}) **9**.

For copper(I) the planar configuration is energetically preferred at the HF and BLYP levels, but not at the MP2 level. In general, the energy difference between the two configurations is small, although the pyramidal one becomes more stable going from Cu to Au. It is thus indicated that inclusion of correlation effects favours a pyramidal C_{3v} symmetry of the trimers. The overlap populations between the metal atoms are in all cases essentially zero or slightly negative, just as for the non-solvated complexes. The attractive force favouring the

bent configuration should therefore be ascribed to electron correlation (vdW, or more precisely, dispersion interaction). The molecules are very likely to be easily angularly deformed because of the small difference in energy. It should also be noted that the optimised I–M–Cl angle deviates slightly from 180° in the pyramidal configuration.

The tetrameric molecules can adopt three different symmetric configurations; tetrahedral (T_d) **10**, square planar (D_{4h}) **11** or square pyramidal (C_{4v}) **12**.

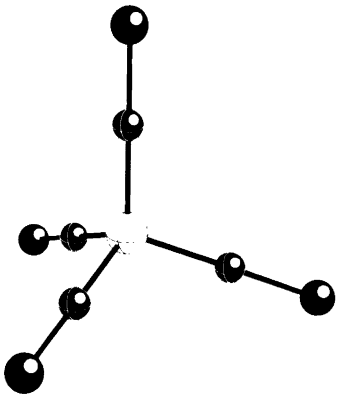

10

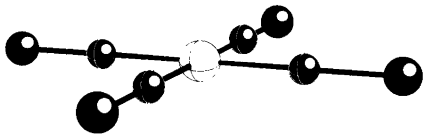

11

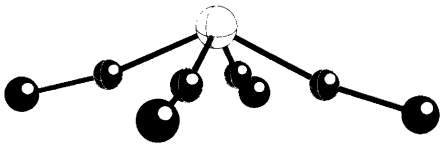

12

For all group 11 metals the configuration of **12** is the energetically favoured one when electron correlation is taken into account (BLYP and MP2 levels). In absence of the recent solid-state structures presented by Schmidbaur and co-workers these results should have been regarded with some suspicion. It should be noted that the $[M_4I]^{3+}$ structural motif exists in some copper(I) and silver(I) iodide compounds as well; in $Ag_2I(NO_3)(s)$ and $Ag_3I(NO_3)_2(s)$ the coordination around I^- is best described as a distorted trigonal prism with four shorter and two longer Ag–I distances,[40,41] and in $RbCu_2I_3(s)$ and $Ag_2IF \cdot H_2O(s)$ pyramidal $[M_4I]^{3+}$ units are linked along one M–M edge into chains of formal $[M_2I]^+$ composition.[31,43] In these compounds the $[M_4I]^{3+}$ pyramids have approximate C_{2v} symmetry, with two longer and two shorter M–M distances. The short M–M distances are essentially equal to the M–I distance, and the $Ag_2IF \cdot H_2O(s)$ was described in terms of $[Ag_2]^{2+}$ pairs.

The energy difference between the T_d and C_{4v} symmetries is very small for the silver system, $[Ag_4ICl_4]^-$, possibly indicating an easy interchange between these configurations. The gold cluster favours the C_{4v} configuration the most, possibly giving support to the claims that relativistic effects enhance the correlation interaction. The relativistic effects are here only included through the use of average relativistic ECPs (i.e. scalar effects). It should be noted that for the corresponding copper system the C_{4v} configuration is almost equally stabilised, although relativistic effects are expected to be much smaller than for gold. Thus we cannot observe any clear relativistic effect going from Cu to Au, although we would expect a difference in performance between a non- and quasi-relativistic ECP for gold. It can also be noted that Au behaves more like Cu than Ag.

It is here also appropriate to highlight the unpredictable behavior of the DFT method (BLYP). These functionals tend to mimic the HF results for the dimers and trimers, but those of MP2 for the tetramers. Therefore, results studying the effects of correlation obtained from DFT methods should be taken with some reservation.

The conversion between T_d and C_{4v} configurations can easily be visualised, **13**, involving the inversion of a ClM–I–MCl pair. The D_{4h} symmetry is thus included only for sake of completeness.

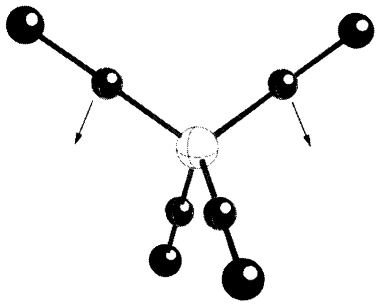

13

Interpretation of correlation effects. The concept of correlation effects may appear somewhat abstract, since they can not easily be visualised in a direct way. It is particularly difficult in the systems studied here, since the metal atoms are connected via a bridging iodide ion. What are the effects of the inclusion of dynamic electron correlation on the direct metal–metal interaction, and what are the effects on the hybridisation on the iodide ion? Although doing relatively advanced calculations, we seem to be confined to a phenomenological explanation: when instantaneous electron correlation is adequately taken into account, the metal–metal separations decrease, producing polymetal complexes with small M–I–M angles.

Much can of course be said of about the level at which correlation has been taken into account. MP2 is known to overestimate the correlation effects when using large-

core ECPs. However, that argument would only be valid for the silver systems (36-electron ECP), for which we observe the smallest correlation effects. A more precise estimation would require the inclusion of metal f-functions and calculations on coupled cluster or configuration interaction levels. However, we must never forget that the largest approximation we make in this study is to 'extract' the polymetal complexes from the ionic media performing the calculations on isolated model systems. With this in mind we believe that the present study is undertaken at an appropriate level, and that the results can be regarded as at least semi-quantative.

The obvious analogy between the $[M_2I]^+$ complexes and H_2O makes the qualitative analysis on extended Hückel level quite informative.[60] As seen in Fig. 2, the preferred bent geometry for the $[M_2I]^+$ ions can be understood as a consequence of a second-order Jahn–Teller interaction between the HOMO of π_u symmetry and LUMO of σ_g symmetry in the linear configuration. The interaction causes a distortion in which one of the π_u components essentially remains unchanged ($1b_1$ in C_{2v}), whereas the s and p orbitals on the iodine atom mix to push the other π_u component ($2a_1$ in C_{2v}) and σ_g ($3a_1$ in C_{2v}) away from each other, thus cancelling the second-order Jahn–Teller instability. The bent geometry in this highly approximate analysis ends up with an optimal M–I–M angle between 90 and 100° for all three coinage metals. The amount of energy stabilisation obtained is inversely correlated to the energy difference between the π_u and σ_g orbitals in the linear configuration (1.9 eV for Cu, 3.9 eV for Ag and 1.1 eV for Au), and consequently the energy differences between the bent and linear configurations follow exactly the same pattern, Au > Cu > Ag, as found in the MP2 calculations. It should also be mentioned that this is purely an effect on the central iodine atom, since all M–M overlap populations are zero also in the most stable bent configuration.

Qualitatively, the same arguments of a second-order Jahn–Teller interaction can be exploited for the $[M_3I]^{2+}$ ions (the HOMO of $1a_2''$ and LUMO of $2a_1'$ symmetry in D_{3h} push the corresponding $2a_1$ and $3a_1$ orbitals apart by s–p mixing on iodine in C_{3v}) and for the $[M_4I]^{3+}$. In

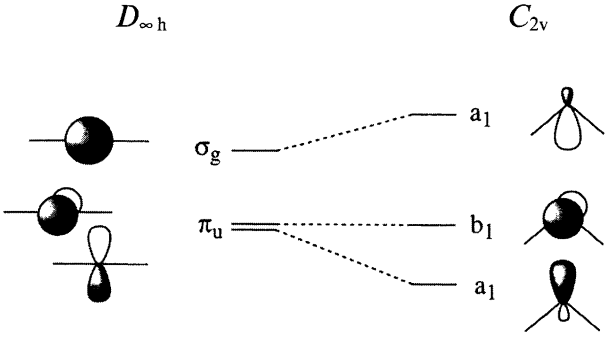

Fig. 2. A schematic view of the cancellation of the second-order Jahn–Teller situation for the linear configuration by s–p mixing on the iodide ion upon bending.

the tetrametal complex the situation is more complicated, starting from a square-planar D_{4h} symmetry, since both distortions to either T_d or C_{4v} symmetries will defuse the near Jahn–Teller degeneracy. The distortion to the C_{4v} configuration is in all important aspects analogous to those for the di- and trimetal complexes. In all cases, the order of energy stabilisation mimics those from *ab initio* calculations: Au > Cu > Ag.

It is clear that bending the M–I–M angles in the polymetal complexes introduces an increase in s–p mixing on the iodine atom also in the more advanced calculations. The fundamental question thus emerges: what is the ultimate cause of the bending distortions we observe; second-order Jahn–Teller or metal–metal dispersion effects? The case can of course be pleaded for both explanations, but from an experimental point of view we must never forget that the biggest approximation in the theoretical description is the full or partial neglect of interactions with the surrounding medium.

Consequences for the interpretation of experimetal results

In the interpretation of the experimental X-ray scattering experiments there were two explanations offered to account for the absence of any Ag–Ag correlation expected from a $[Ag_4I]^{3+}$ (or $[Ag_4Br]^{3+}$) cluster: (1) absence of definite energy minima, thus producing no well defined time and space average features in the radial distribution functions ('silver ions floating on the surface of the large halide anions'); (2) a misinterpretation of the thermodynamic data due to changes in activity factors, so that the stepwise complex formation with Ag^+ may stop at three per halide ion ($[Ag_3X]^{2+}$) instead of four ($[Ag_4X]^{3+}$). If the trimeric silver complex adopts a nearly perfect pyramidal structure, the Ag–Ag distances would coincide with the Ag–X distances and thus give rise to only one peak in the difference radial distribution functions.

The first model was preferred for three reasons. Firstly, it is unlikely that the Ag–Ag separations coincide perfectly not only with Ag–I distances in the iodide system but also with the Ag–Br ones in the bromide system. Secondly, a nearly perfect pyramidal $[Ag_3I]^{3+}$ configuration ought to give rise to a strong Raman-active vibrational band from the breathing mode, but only a weak polarised band at about 140 cm^{-1} is observed in the Raman spectra of highly concentrated solutions and melts (generally, the silver halide glasses, melts and solutions tend to reveal very little information when exposed to various spectroscopic methods).[61] Thirdly, there is a vast number of Ag^+-conducting glasses with almost identical AgX–AgOx (Ox = oxoanion) compositions as the molten nitrates studied by us. The local structure in the analogous glass systems is described in terms of silver iodide clusters. These circumstances, of course, offer an exciting link between the macroscopic (bulk) property of silver ion conductivity and the implicated microscopic (molecular) flexbility for $[Ag_4I]^{3+}$ emerging from this study. However, it should be

emphasised that the larger degree of flexibility found for the polysilver complexes is only of a quantitative nature, and there is no qualitative difference in the bonding scheme between silver and copper or gold.

We can thus conclude that the present theoretical study lends support to a model based on intramolecular mobility of the silver ions coordinated to halide centres; the silver ions can be visualised as 'floating' on the electron surface of the central halide ion. Currently, theoretical studies on extended systems aiming at the estimation of the diffusion and conductivity properties of the coinage metal ions in halide compounds are being pursued.

Acknowledgements. This work has been supported by the Swedish Natural Science Research Council, DGES (grant PB95-0848-C02-01), and CIRIT (grant 1995SGR-00421). We are grateful to S. Alvarez for many helpful comments on this work.

References

1. Leden, I. *Acta Chem. Scand. 10* (1956) 540; 812.
2. Lieser, K. H. *Z. Anorg. Allg. Chem. 292* (1957) 97; *304* (1960) 296; *305* (1960) 133.
3. Holmberg, B. *Acta Chem. Scand. 27* (1973) 875; 3550; 3657.
4. Holmberg, B. *Acta Chem. Scand., Ser. A 30* (1976) 797.
5. Yamaguchi, T., Johansson, G., Holmberg, B., Maeda, M. and Ohtaki, H. *Acta Chem. Scand., Ser. A 38* (1984) 437.
6. Holmberg, B. and Johansson, G. *Acta Chem. Scand., Ser. A 37* (1983) 367.
7. See for instance: (a) Grohmann, A., Riede, J. and Schmidbaur, H. *Nature (London) 345* (1990) 140. (b) Schmidbaur, H. *Gold Bull. 23* (1990) 11. (c) Bommers, S., Beruda, H., Dufour, N., Paul, M., Schier, A. and Schmidbaur, H. *Chem. Ber. 128* (1995) 137. (d) Sladek, A., Angermaier, K. and Schmidbaur, H. *J. Chem. Soc., Chem. Commum.* (1996) 1959.
8. Bowmaker, G. A., Pabst, M., Rösch, N. and Schmidbaur, H. *Inorg. Chem. 32* (1993) 880.
9. Yam, V. W.-W., Lee, W.-K., Cheung, K.-K., Crystall, B. and Phillips, D. *J. Chem. Soc., Dalton Trans.* (1996) 3283.
10. Yam, V. W.-W., Lo, K. K.-W., Wang, C.-R. and Cheung, K.-K. *Inorg. Chem. 35* (1996) 5116.
11. Some examples are: (a) Li, J. and Pyykkö, P. *Inorg. Chem. 32* (1993) 2630. (b) Pyykkö, P. and Runeberg, N. *J. Chem. Soc., Chem. Commun.* (1993) 1812. (c) Pyykkö, P., Li, J. and Runeberg, N. *Chem. Phys. Lett. 218* (1994) 133. (d) Häberlen, O. D., Schmidbaur, H. and Rösch, N. *J. Am. Chem. Soc. 116* (1994) 8241. (e) Burdett, J. K., Eisenstein, O. and Schweizer, W. B. *Inorg. Chem. 33* (1994) 3261. (f) Pyykkö, P., Angermaier, K., Assmann, B. and Schmidbaur, H. *J. Chem. Soc., Chem. Commun.* (1995) 1889. (g) Chung, S.-C., Krüger, S., Schmidbaur, H. and Rösch, N. *Inorg. Chem. 35* (1996) 5387.
12. Pyykkö, P. *Chem. Rev. 97* (1997) 597.
13. Schäfer, A., Huber, C., Gauss, J. and Alrichs, R. *Theor. Chim. Acta 87* (1993) 29.
14. Schäfer, A. and Alrichs, R. *J. Am. Chem. Soc. 116* (1994) 10686.
15. Dehnen, S., Schäfer, A., Fenske, D. and Alrichs, R. *Angew. Chem., Int. Ed. Engl. 33* (1994) 746.
16. Alemany, P., Novoa, J. J. and Bengtsson, L. A. *Int. J. Quantum. Chem. 52* (1994) 1.
17. Bagaturyants, A. A., Safonov, A. A., Stoll, H. and Werner, H.-J. *In press.*
18. Frisch, M. J., Trucks, G. W., Schlegel, H. B., Gill, P. M. W., Johnson, B. G., Robb, M. A., Cheeseman, J. R., Keith, T. A., Petersson, G. A., Montgomery, J. A., Raghavshari, K., Al-Laham, M. A., Zakrzewski, V. G., Ortiz, J. V., Foresman, J. B., Cioslowski, J., Stefanov, B., Nanayakkara, A., Challacombe, M., Peng, C. Y., Ayala, P. Y., Chen, W., Wong, M. W., Andres, J. L., Replogle, E. S., Gomperts, R., Martin, R. L., Fox, D. J., Binkley, J. S., Defrees, D. J., Baker, J., Stewart, J. P., Head-Gordon, M., Gonzalez, C. and Pople, J. A. *Gaussian 92/94*, Gaussian Inc., Pittsburgh, PA 1995.
19. Hay, P. J. and Wadt, W. R. *J. Chem. Phys. 82* (1985) 270; 284; 299.
20. Dunning T. H. Jr. and Hay, P. J. In Schaefer, H. F. III, Ed., *Modern Theoretical Chemistry*, Plenum, New York 1976, pp. 1 -28.
21. Some recent articles on ECP performance: (a) Frenking, G., Antes, I., Böhme, M., Dapprich, S., Ehlers, A. W., Jonas, V., Neuhaus, A., Veldkamp, A. and Vyboishchikov, S. F. In Lipkowitz, K. B. and Boyd, D. B., Eds., *Reviews in Computational Chemistry*, VCH, New York 1995, Vol. 8. (b) Klobukowski, M. *Theor. Chim. Acta 83* (1992) 239. (c) Schwerdtfeger, P., Fischer, T., Dolg, M., Igel-Mann, G., Nicklass, A., Stoll, H. and Haaland, A. *J. Chem. Phys. 102* (1995) 2050. (d) Leininger, T., Nicklass, A., Stoll, H., Dolg, M. and Schwerdtfeger, P. *J. Chem. Phys. 105* (1996) 1052. (e) Smart, B. A. and Schiesser, C. H. *J. Comput. Chem. 16* (1995) 1055.
22. Ernzerhof, M., Perdew, J. P. and Burke, K. In *Topics in Current Chemistry 180*, Springer-Verlag, Berlin 1996, p. 2.
23. Becke, A. D. *Phys. Rev., Ser. A 38* (1988) 3098.
24. Lee, C., Yang, W. and Parr, P. G. *Phys. Rev., Ser. B 37* (1988) 785; Mielich, B., Savin, A., Stoll, H. and Preuss, H. *Chem. Phys. Lett. 157* (1989) 200.
25. Jansen, M. *Angew. Chem. Int. Ed. Engl. 26* (1987) 1098.
26. Hay, P. J., Thibeault, J. C. and Hoffmann, R. *J. Am. Chem. Soc. 97* (1975) 4884.
27. Canadell, E. and Eisenstein, O. *Inorg. Chem. 22* (1983) 2398.
28. Manson, E. L. *J. Chem. Phys. 62* (1975) 4796.
29. Yude, Y., Boysen, H. and Schulz, H. *Z. Kristallogr. 191* (1990) 79.
30. Eriksson, L, Wang, P. and Werner, P.-E. *Z. Kristallogr. 197* (1991) 235.
31. Pfitzner, A. and Freudenthaler, E. *Z. Kristallogr. 210* (1995) 59.
32. (a) Asplund, M., Jagner, S. and Nilsson, M. *Acta Chem. Scand., Ser. A 36* (1982) 751. (b) Asplund, M. and Jagner, S. *Acta Chem. Scand., Ser. A 38* (1984) 297. (c) Asplund, M. and Jagner, S. *Acta Chem. Scand., Ser. A 38* (1984) 411.
33. Andersson, S., Helgesson, G., Jagner, S. and Olson, S. *Acta Chem. Scand. 43* (1989) 946.
34. Persson, I., Sandström, M., Steel, A. T., Zapatero, M. J. and Åkesson, R. *Inorg. Chem. 30* (1991) 4075.
35. Barrow, R. F., Clements, R. M. and Wright, C. V. *Trans. Faraday Soc. 63* (1967) 2874.
36. Hoshino, S., Sakuma, T. and Fujii, Y. *Solid State Commun. 22* (1977) 763.
37. Cava, R. J., Reidinger, F. and Wünsch, B. J. *Solid State Commun. 24* (1977) 411.
38. Kasper, J. S. and Browall, K. W. *J. Solid State Chem. 13* (1975) 49.
39. Browall, K. W., Kasper, J. S. and Wiedmeier, H. *J. Solid State Chem. 10* (1974) 20.
40. Persson, K. *Acta Crystallogr., Sect. B 35* (1979) 302.
41. Birnstock, R. and Britton, D. *Z. Kristallogr. 132* (1970) 87.
42. Persson, K. and Holmberg, B. *Acta Crystallogr., Sect. B 38* (1982) 904.
43. Persson, K. and Holmberg, B. *J. Solid State Chem. 42* (1982) 1.

44. Helgesson, G. and Jagner, S. *Inorg. Chem. 30* (1991) 2574.
45. Helgesson, G. and Jagner, S. *J. Chem. Soc., Dalton Trans.* (1990) 2413.
46. Olson, S., Helgesson, G. and Jagner, S. *Inorg. Chim. Acta 217* (1994) 15.
47. Nilsson, K. and Persson, I. *Acta Chem. Scand., Ser. A 41* (1987) 139.
48. Johansson, M. and Persson, I. *Inorg. Chim. Acta 130* (1987) 215.
49. Jagodzinski, H. *Z. Kristallogr. 112* (1959) 80.
50. Helgesson, G. and Jagner, S. *Acta Chem. Scand., Ser. A 41* (1987) 556.
51. Wells, A. F. *Structural Inorganic Chemistry*, 5th Edn., Oxford University Press, Oxford 1984, p. 444.
52. Fourcroy, P. H., Carré, D. and Rivet, J. *Acta Crystallogr., Sect. B 34* (1978) 3160.
53. (a) Chadha, G. K. *Z. Kristallogr. 139* (1974) 147. (b) Sarna, I., Chadha, G. K. and Trigunayat, G. C. *Z. Kristallogr. 139* (1974) 147.
54. Bengtsson, L. and Holmberg, B. *Acta Chem. Scand. 44* (1990) 447.
55. (a) Jeffrey, G. A. and Vlasse, M. *Inorg. Chem. 6* (1967) 396. (b) Schwarzenbach, D. *Z. Kristallogr. 128* (1969) 97.
56. Persson, K. and Holmberg, B. *Acta Crystallogr., Sect. B 38* (1982) 900.
57. Köhler, K., Breitinger, D. and Thiele, G. *Angew. Chem. 86* (1974) 861.
58. Sandström, M. *Acta Chem. Scand., Ser. A 32* (1978) 627.
59. Bengtsson, L., Holmberg, B., Persson, I. and Iverfeldt, Å. *Inorg. Chim. Acta 146* (1988) 233.
60. Albright, T. A., Burdett, J. K. and Whangbo, M. H. *Orbital Interactions in Chemistry*, Wiley, New York 1985.
61. Bengtsson-Kloo, L. *Unpublished results.*

Received September 12, 1997.